Since January 2020 Elsevier has created a COVID-19 resource centre with free information in English and Mandarin on the novel coronavirus COVID-19. The COVID-19 resource centre is hosted on Elsevier Connect, the company's public news and information website.

Vaccine 32 (2014) 5740–5748

Contents lists available at ScienceDirect

Vaccine

journal homepage: www.elsevier.com/locate/vaccine

Attenuation of highly pathogenic porcine reproductive and respiratory syndrome virus by inserting an additional transcription unit

Lianghai Wang[a,b,c,1,2], Jun Hou[a,b,c,1,2], Li Gao[a,b,c], Xue-kun Guo[a,b,c], Zhibin Yu[a,b,c], Yaohua Zhu[a,b,c], Yihao Liu[a,b,c], Jun Tang[a,d], Hexiao Zhang[e], Wen-hai Feng[a,b,c,*]

[a] State Key Laboratory of Agrobiotechnology, China Agricultural University, Beijing 100193, China
[b] Ministry of Agriculture Key Laboratory of Soil Microbiology, China Agricultural University, Beijing 100193, China
[c] Department of Microbiology and Immunology, College of Biological Sciences, China Agricultural University, Beijing 100193, China
[d] Department of Basic Veterinary Medicine, College of Veterinary Medicine, China Agricultural University, Beijing 100193, China
[e] Beijing Entry-Exit Inspection and Quarantine Bureau, Beijing 100026, China

ARTICLE INFO

Article history:
Received 3 July 2014
Received in revised form 6 August 2014
Accepted 15 August 2014
Available online 26 August 2014

Keywords:
HP-PRRSV
Additional transcription unit
Genome instability
Attenuation

ABSTRACT

Transcription regulatory sequences (TRSs) play a key role in the synthesis of porcine reproductive and respiratory syndrome virus (PRRSV) subgenomic mRNAs, which resembles similarity-assisted RNA recombination. In this study, genome instability was found when a highly pathogenic PRRSV (HP-PRRSV) strain was inserted by an additional transcription unit in which a foreign gene GFP was expressed from TRS2 while a copy of TRS6 drove ORF2a/b transcription. Structural protein gene-deleted genomes resulted from enhanced RNA recombinations were identified in the recombinant virus rHV-GFP. Moreover, rHV-GFP replicated slower than parental viruses, and caused less cell death in porcine alveolar macrophages. Pigs infected with rHV-GFP survived with no or mild syndromes, whereas all pigs infected with parental viruses died within 12 days. Our data showed that additional transcription unit insertion could confer genome instability and attenuation of HP-PRRSV.

1. Introduction

Arterivirus and coronavirus generate a 3′ co-terminal nested set of subgenomic mRNAs during virus replication. The subgenomic transcripts also contain a common 5′ leader sequence, which is derived from the 5′ end of the genomic RNA. Their synthesis involves a discontinuous transcription process that resembles similarity-assisted RNA recombination [1]. Transcription regulatory sequences (TRSs) consisting of conserved hexanucleotide motif and poorly conserved flanking sequences forming secondary structures are present at the 3′ end of the common leader (leader TRS) and upstream of each structural protein gene (body TRSs), and play a key role in the synthesis of subgenomic mRNAs [1,2]. The body TRSs could act as attenuation signals during minus-strand RNA synthesis, and then the nascent minus strand would be redirected to the 5′-proximal region of the template by a base-pairing interaction between the leader TRS and the antisense copy of the body TRSs. Then the completed subgenomic-length minus strands would serve as templates for the transcription of subgenomic mRNAs [1,3].

Porcine reproductive and respiratory syndrome virus (PRRSV) is an important arterivirus, causing respiratory diseases in piglets and severe reproductive failures in sows [4,5]. In May 2006, highly pathogenic PRRSV (HP-PRRSV), which was observed with a unique molecular hallmark namely a discontinuous deletion of 30 amino acids in nonstructural protein 2, emerged in China. HP-PRRSV infection is characterized by high fever, high morbidity, and high mortality in pigs of all ages [6–8]. In the past 5 years, HP-PRRSV has reemerged several times and caused immense economic losses for the swine industry in China.

Reverse genetics system provides a powerful tool to dissect the functions of viral proteins in viral life cycle and pathogenicity by gene manipulation. However, overlapped ORFs make it difficult to

* Corresponding author at: State Key Laboratories of Agrobiotechnology, Department of Microbiology and Immunology, College of Biological Sciences, China Agricultural University, Beijing 100193, China. Tel.: +86 10 62733335; fax: +86 10 62732012.
E-mail address: whfeng@cau.edu.cn (W.-h. Feng).
[1] These authors contributed equally to this work.
[2] Current address: Shihezi University School of Medicine, Shihezi, Xinjiang 832002, China.

http://dx.doi.org/10.1016/j.vaccine.2014.08.036
0264-410X/

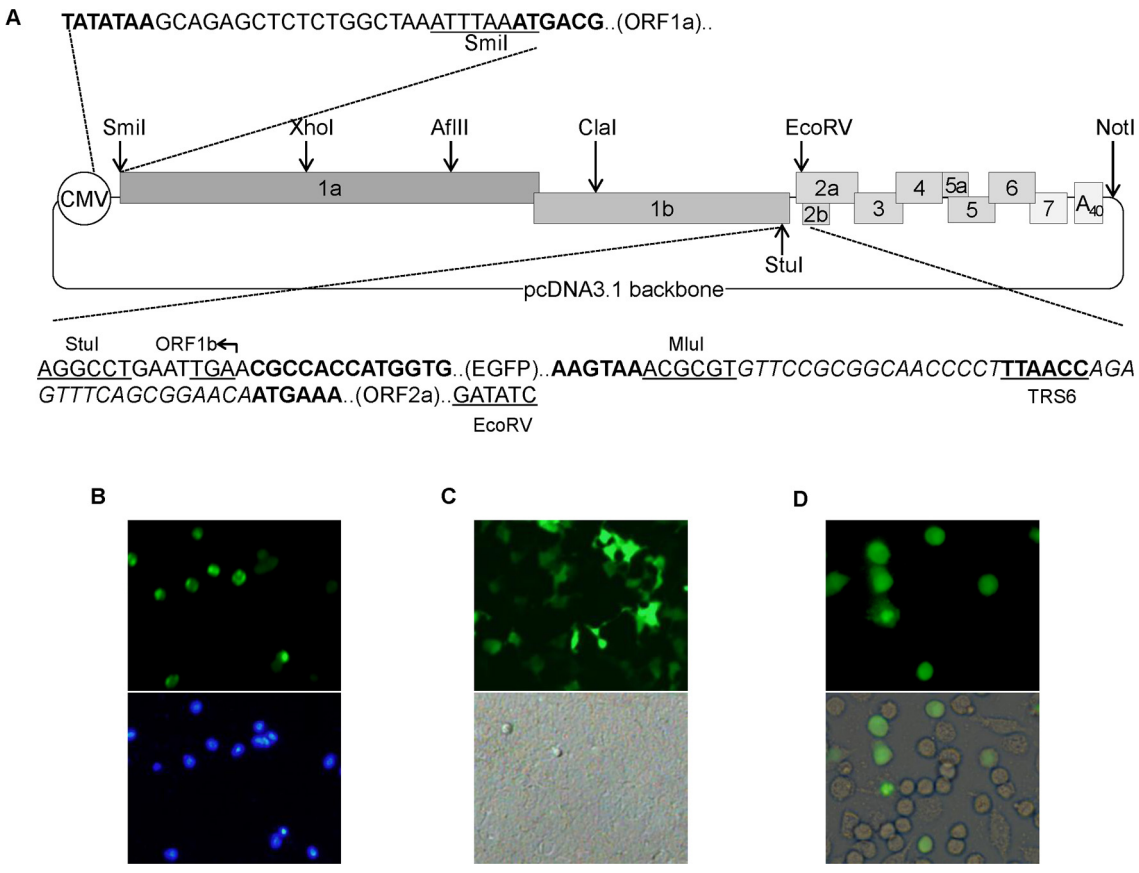

Fig. 1. Construction of a recombinant HP-PRRSV expressing an additional transcription unit (rHV-GFP). (A) Strategy for the construction of the recombinant cDNA clone. Five overlapping fragments amplified from the HV genome were ligated into the modified pcDNA3.1 vector using the listed restriction enzyme cleavage sites. GFP gene and a copy of TRS6 were introduced into the non-coding region between ORF1b and ORF2a using restriction sites Stu I and Mlu I. TTAACC, the core hexanucleotide of TRS6; the sequence in italic indicates its flanking sequences. (B) The plasmid containing assembled HV genome was transfected into 293FT cells. The reused virus rHV was passaged on PAMs and immunofluorescence assay was performed for virus detection. Magnification, 200×. (C) The recombinant cDNA clone containing GFP gene and a copy of TRS6 was transfected into 293FT cells and directly examined for GFP expression at 48 h post transfection under an immunofluorescence microscope. Magnification, 200×. (D) rHV-GFP was serially passaged on PAMs and green fluorescence was directly examined under an immunofluorescence microscope. Magnification, 400×.

manipulate PRRSV genome [9]. Recently, PRRSV gene expression vectors capable of expressing a foreign gene from an additional transcription unit were generated by inserting a copy of the transcription regulatory sequence for ORF6 (TRS6) [10–13]. This novel approach was used to construct recombinant viruses expressing antiviral cytokines as adjuvants to overcome immune subversion of PRRSV and enhance the viral specific immune response following vaccination [13], or expressing reporter proteins to monitor virus replication, as well as elucidating the role of host factors and screening for novel antiviral drugs [11,13]. This PRRSV reverse genetics system may also function as a vector for development of recombinant multivalent vaccines against swine diseases by encoding immunogenic antigens from other swine pathogens [10]. The inserted foreign gene was supposed to be tolerated by the virus and could be stably expressed in cell culture. In this study, a recombinant HP-PRRSV expressing an additional transcription unit (rHV-GFP) was constructed. RNA recombination resulted from the additional transcription unit insertion conferred high attenuation both *in vitro* and *in vivo*.

2. Materials and methods

2.1. Cells and virus

Porcine alveolar macrophages (PAMs) were collected by post-mortem lung lavage of 8-week-old specific-pathogen-free pigs, and maintained in RPMI 1640 supplemented with 10% FBS [14]. Cells of 293FT line (Invitrogen) were cultured in DMEM containing 10% FBS. HP-PRRSV strain HV (GenBank accession no. JX317648) was used in this study [15]. Viruses were propagated and titrated on PAMs.

2.2. Construction of a full-length cDNA clone

The assembly strategy is illustrated in Fig. 1. Briefly, viral RNA was extracted and reverse transcribed. Then, five overlapping fragments spanning appropriate restriction sites were amplified, and cloned into pMD®18-T vector. Primer sequences were listed in Table 1. Eukaryotic expression vector pcDNA3.1(+) was modified into backbone for assembly. The number of nucleotides between the TATA box and the viral genome was adjusted to 24 as described previously [16]. The plasmid containing assembled genome of HV (pcDNA3.1-HV) was transfected into 293FT cells. Cell culture supernatant obtained at 48 h post transfection was inoculated on PAMs and immunofluorescence assay was performed for virus detection [17]. The rescued virus was designated as rHV.

2.3. Insertion of an additional transcription unit

Enhanced green fluorescent protein (EGFP) gene including Kozak consensus translation initiation site was amplified from pEGFP-N1 vector using primer set of StG-F (containing a StuI site) and StG-R (containing a MluI site). TRS6 or TRS2 sequence was amplified using primer set of TRS6-F or TRS2-F (containing a MluI site) and HV4-R (containing an EcoRV site). The amplification

Table 1
Primer sequences.

Primer	Sequence (5′–3′)	Use
3.1-F	AGATCGATGATATCGCGGCCGCCTCGACTGTGCCTTCTA	pcDNA3.1 modification
3.1-R	TAAGCGCTCGAGCCATTTAAATTTAGCCAGAGAGCTCTGC	pcDNA3.1 modification
HV1-F	TAAATTTAA ATGACGTATAGGTGTTGGCTCT	Fragment clone
HV1-R	GCGTGCGAGGTAACATCA	Fragment clone
HV2-F	TTCTCCCAAAGATGATTCTCG	Fragment clone
HV2-R	GGCAGCGGTACTTAAACAAG	Fragment clone
HV3-F	GCCCTTAACAGAAACAGATGG	Fragment clone
HV3-R	TACGACGGTAGATGCTCCTC	Fragment clone
HV4-F	GGGAAGAAGAAGACTAGGACAAT	Fragment clone
HV4-R	TCAGGGTGAACGGTAGAGC	Fragment clone
HV5-F	GCCCTGTCATTGAACCAACT	Fragment clone
HV5-R	TTATTAGCGGCCGCTTTTTTTTTTTTTTTTTTTTTTTTTTTTTTTTTTTTTTTTTTTTAATTACGGCCGCATGGTT	Fragment clone
StG-F	TTTAGGCCTGAATTGAA CGCCACCATGGTGAGCAA	GFP insertion
StG-R	GCGACGCGTTTACTTGTACAGCTCGTCCAT	GFP insertion
TRS6-F	GCGACGCGTGTTCCGCGGCAACCCCTTTAACCAGAGTTTCAGCGGAACAATGAAATGGGGTCTATGCAAAGCCTCTTTGACA	TRS6 insertion
TRS2-F	AATTACGCGTTTTCCCCCGGGCCCTGTCATTGAACCAACTTTAGGCCTGAATTGAAATGAAATGGGGTCTATGC	TRS2 insertion
ORF1b-F	AGGATTACAATGATGCGTTTCG	Gene-deletion detection
ORF7-F	AAACCAGTCCAGAGGCAAGG	ORF7 detection
ORF7-R	GCCGCTCACTAGGGGTAAAG	Gene-deletion and ORF7 detection
ORF3-F	CTGGTTGGCGTTCCTGTCC	ORF3 detection
ORF3-R	GGTGGCGTTATCCCCGTC	ORF3 detection

F denotes a forward primer; R denotes a reverse primer.

products were cut by MluI and ligated using T4 DNA ligase. Then PCR was performed using the ligation product as templates and primer set of StG-F and HV4-R. The PCR products were digested with StuI–EcoRV, ligated to the shuttle plasmid which contains the fourth fragment of HV, and further inserted into pcDNA3.1-HV. After insertion, the plasmid was transfected into 293FT cells and GFP expression was examined under an immunofluorescence microscope. Cell culture supernatants were serially passaged on PAMs to assess the stability of the inserted GFP. The rescued virus was designated as rHV-GFP (TRS6 inserted) or rHV-GFP-TRS2 (TRS2 inserted).

2.4. Identification of RNA recombination

Viral RNAs isolated from virus stocks were reverse transcribed with random 6 mers. Then PCR was performed using primer pairs spanning ORF1b through ORF7. Amplicons were gel-purified and sub-cloned into pMD®18-T vector, and were then sequenced. In the case of rHV-GFP, RNA secondary structures of the deletion mutants were predicted by using the Mfold web server under default folding conditions (http://mfold.rit.albany.edu/?q=mfold/RNA-Folding-Form) [18] and drew by RNAVIZ version 2 [19].

The ratio of RNA recombination was analyzed by SYBR-green based real-time PCR. Briefly, PAMs were inoculated with HV or rHV-GFP, and then the cell culture supernatant was harvested at 48 h post-infection (h.p.i.). Viral RNA was extracted and reverse transcribed. ORF3 (existed only in non-deleted viruses) copy numbers were normalized by comparing to ORF7 (existed in all viruses) copy numbers and expressed relative to that of HV.

2.5. In vitro characterization of rHV-GFP

rHV-GFP attachment, internalization, and replication were analyzed as described previously with modifications [20]. To determine attachment and internalization, PAMs were inoculated with HV or rHV-GFP at an MOI of 1.0 at 4 °C for 1 h. Then the inoculums were removed and cells were washed with cold medium to remove residual viruses before being replaced with pre-warmed medium. After 3 h incubation at 37 °C, cellular RNA was isolated and reverse transcribed. Then PCR was performed to identify gene-deleted genomes. rHV-GFP replication was analyzed by detecting the expression of GFP and viral N protein using immunofluorescence assay at 24 h.p.i.

For the growth kinetics of the rescued viruses, PAMs were inoculated with either HV, rHV, or rHV-GFP at an MOI of 0.1. Aliquots of the cell culture supernatant were harvested at the indicated time points post-infection. Viral titration was performed by a standard $TCID_{50}$ assay as described previously [21]. Cell death rates were determined by trypan blue exclusion dye staining at 36 h.p.i..

2.6. Animal studies

Thirteen 4-week-old healthy conventional Large White–Dutch Landrace crossbred pigs were obtained from a pig farm that was negative for PRRSV and PCV2 infections. Pigs were randomly divided into three groups and housed in separate rooms. Then pigs were intranasally inoculated with 2 ml of virus stock containing 10^7 $TCID_{50}$/ml (three pigs for HV, three pigs for rHV, and seven pigs for rHV-GFP). The animals were monitored daily for clinical signs. Rectal temperatures were measured every other day. Serum samples were collected twice a week and used for virus titration by real-time PCR using ORF7 specific primers. Pigs were humanely euthanized and necropsied when animal welfare was compromised. Three of rHV-GFP infected pigs were euthanized at 14 days post inoculation (d.p.i.), while the other four pigs were euthanized at the end of the experiment (28 d.p.i.). Tissues of the pigs euthanized at 14 d.p.i. or earlier due to severe disease were collected and either fixed in 10% neutral-buffered formalin and routinely processed for histological examination, or snap-frozen in liquid nitrogen and stored at −80 °C for RNA isolation. Microscopic lesions were evaluated by veterinary pathologists blinded to the treatment status.

All animals studies were performed in accordance with the guidelines of China Agricultural University Institutional Animal Care and Use Committee (ID: SKLAB-B-2010-003), and approved by animal welfare committee of China Agricultural University.

2.7. Statistical analysis

All experiments were performed with at least three independent replicates, and data represent means ± SD. Results were analyzed using *Student's t-test*. Differences were considered to be statistically significant if the p value was less than 0.05.

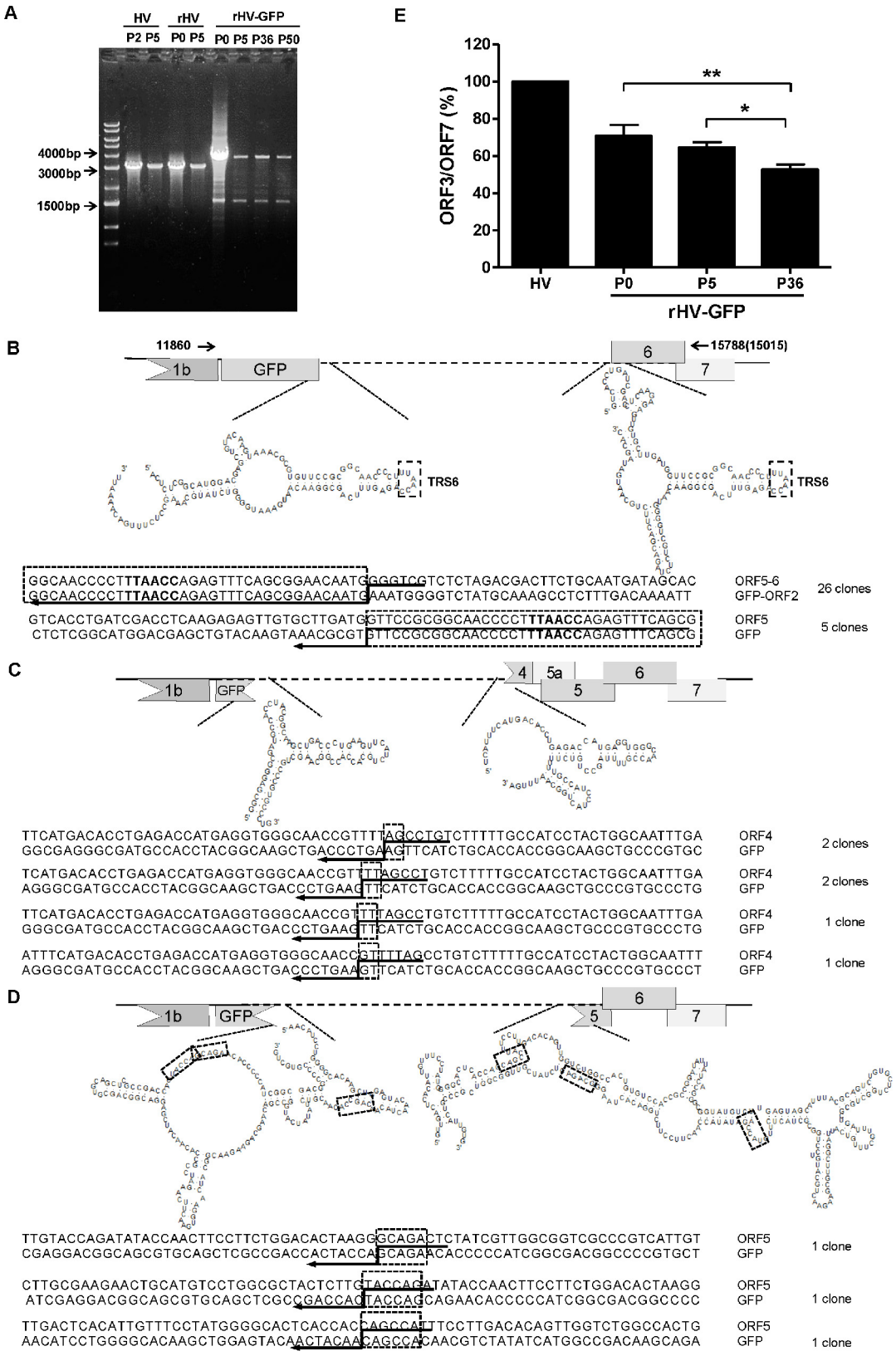

Fig. 2. Identification of RNA recombination in rHV-GFP. (A) RNA recombination was examined by PCR using primer pairs spanning ORF1b through ORF7 (nucleotides 11947–15015 according to HV and rHV genome, and nucleotides 11947–15788 according to rHV-GFP genome). P0, passage 0. (B–D) Schematic representation of the deletion mutants identified in the amplification products by nucleotide sequencing. PCR products were gel-purified and sub-cloned for sequencing analysis. RNA secondary structures of the deletion mutants were predicted by using the Mfold web server and drew by RNAVIZ version 2. Postulated polymerase strand switching during replication is indicated by the arrow. RNA recombination spots could be at anywhere within the consecutive nucleotides been boxed. The nucleotides in bold represent TRS6 sequence. (E) The ratio of rHV-GFP with full-length genome was analyzed by SYBR-green based real-time PCR. ORF3 copy numbers were normalized by comparing to ORF7 copy numbers and expressed relative to that of HV. $^{**}p < 0.01$, $^{*}p < 0.05$.

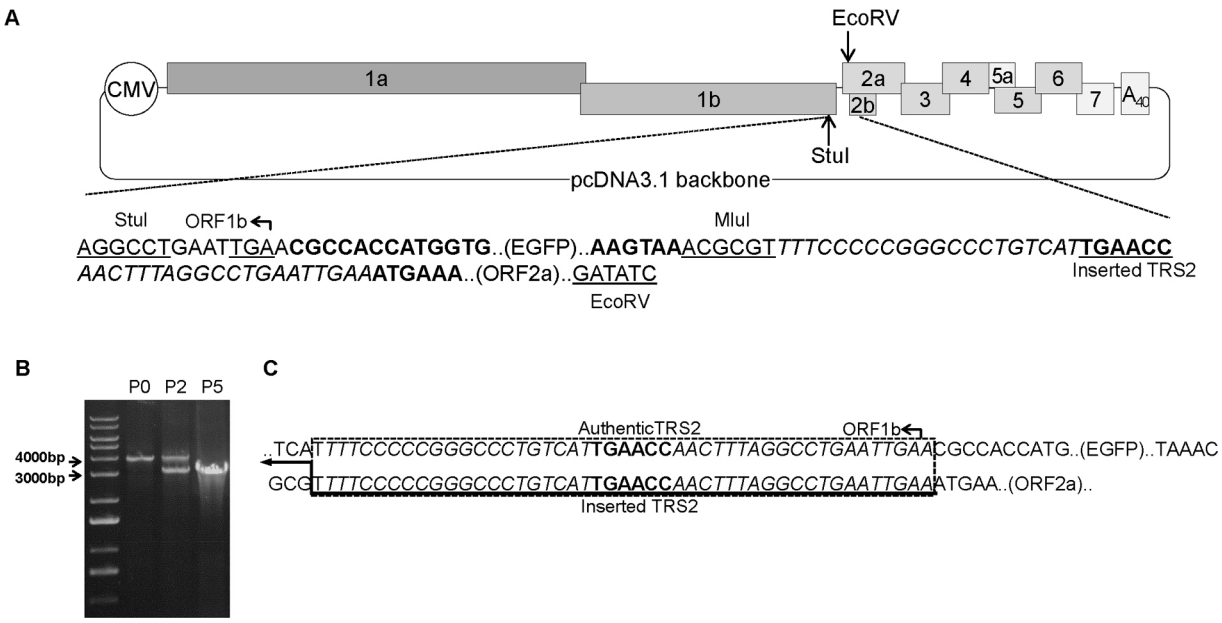

Fig. 3. Abrogation of viral gene deletion in rHV-GFP-TRS2. (A) Schematic representation of the recombinant cDNA clone containing GFP gene and an additional TRS2. The hexanucleotide motif was in bold and its flanking sequences were in italic. (B) RNA recombination was examined by PCR using primer pairs spanning ORF1b through ORF7 (nucleotides 11947–15015 according to HV genome, and nucleotides 11947–15788 according to rHV-GFP-TRS2 genome). P0, passage 0. (C) Sequence of the additional transcription unit inserted region. Postulated polymerase strand switching during replication is indicated by the arrow. RNA recombination spots could be at anywhere within the consecutive nucleotides been boxed.

3. Results

3.1. Construction of a recombinant HP-PRRSV expressing an additional transcription unit (rHV-GFP)

HP-PRRSV strain HV was isolated from a piglet with respiratory symptoms in China in 2007. Five overlapping fragments were sequentially assembled into modified eukaryotic expression vector pcDNA3.1(+) (Fig. 1A). BHK-21 and Marc-145 cell lines are previously used for PRRSV rescue [22]. In this study, we used 293FT cell line to rescue PRRSV. The full-length cDNA clone was transfected into 293FT cells and then the cell culture supernatant was passaged on PAMs. Immunofluorescence assay demonstrated that viable viruses (rHV) could be successfully rescued (Fig. 1B). Then, an additional transcription unit which a foreign gene GFP was expressed from TRS2 while a copy of TRS6 drove ORF2a/b transcription was inserted in the region between the non-structural and structural genes. At 48 h post transfection, a high percentage of GFP-positive cells could be observed under an immunofluorescence microscope (Fig. 1C), indicating that 293FT cell is appropriate for PRRSV packaging. Moreover, green fluorescence could still be observed when the rescued recombinant virus (rHV-GFP) was passaged on PAMs for at least 50 passages (Fig. 1D).

3.2. Identification of RNA recombination in rHV-GFP

Various factors can influence RNA recombination, including the sequence similarity between the nascent and the acceptor nucleic acid molecules, the kinetics of transcription, and secondary structure in the RNA that may promote template switching through stalling of the RNA polymerase during replication and then facilitating the transfer onto the acceptor RNA [23,24]. Although the foreign gene GFP seemed to be stably expressed, homologous RNA recombination was predicted to happen between the additional TRS6 and the authentic TRS6. RNA recombination was verified by PCR using primer pairs spanning ORF1b through ORF7 (Fig. 2A). The sizes of amplification products from HV and rHV cDNA were exactly the same as predicted (about 3.1 kb). Whereas two bands were observed in the products generated from rHV-GFP cDNA: a large band which was about 3.8 kb including the inserted GFP gene (about 0.7 kb), and a small band which was about 1.5 kb. The small band was gel-purified and sub-cloned. Sequencing analysis of forty clones showed that they were a mixture of RNA recombination products (Fig. 2B–D). Thirty-one clones were identified as homologous recombinations between the additional TRS6 and the authentic TRS6 (which have the same primary sequences and local secondary RNA structures), resulting in an ORF2-ORF5 deletion as predicted (Fig. 2B). Novel RNA recombination was also found between the inserted GFP gene and ORF4, in which similar hairpin structures were found, and six clones were identified to have deletions including part of the GFP gene, ORF2-3, and part of ORF4 (Fig. 2C). Another three clones had recombinations between GFP and ORF5 (there are weak primary sequence similarity and higher order RNA structures existed in them), resulting in the deletion of partial GFP, ORF2-4, and partial ORF5 (Fig. 2D). We proposed that the replicase was attenuated at one of these secondary structures in the 3′-proximal part of the genome, following a base-pairing interaction, and then it could transfer onto the upstream region of the template which contained a hairpin structure for retargeting of RdRp and nascent strand. Thus, truncated viral genomes were continuously generated by RNA recombination during virus replication. Then, real-time PCR was performed to quantify the proportion of gene-deleted viruses. As shown in Fig. 2E, about 70.7% of rHV-GFP in the cell culture supernatant of transfected 293FT cells had full-length genome (29.3% viruses were gene-deleted). Complete viruses gradually decreased when rHV-GFP was serially passaged on PAMs, and the rate declined to about 52.8% at passage 36 (47.2% viruses were gene-deleted), which was significantly lower than that of passage 0 and passage 5, indicating that deletion mutants were gradually accumulated. However, as only a portion of the genome has been evaluated for recombination, small deletions could have been overlooked, and the proportion of gene-deleted virus is a minimum estimate.

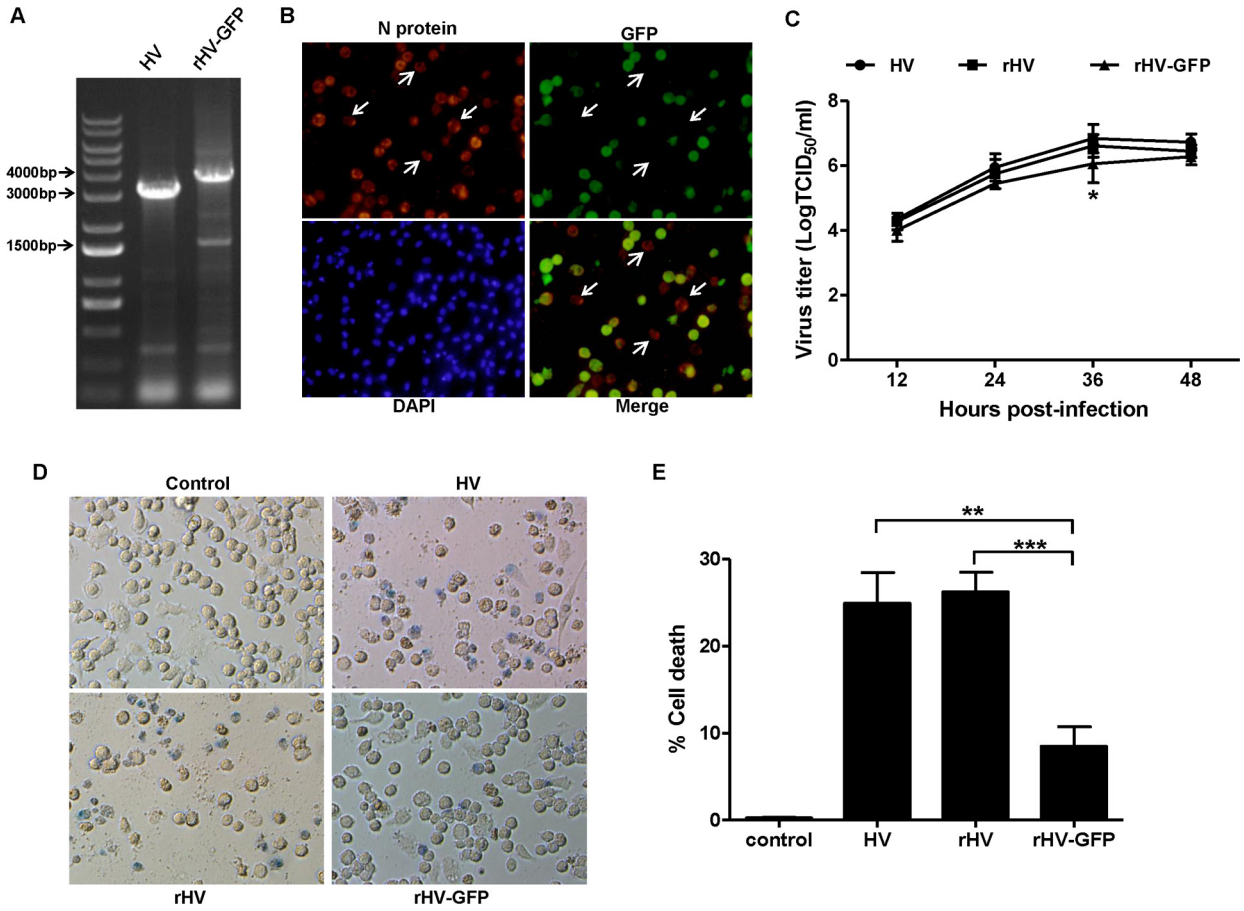

Fig. 4. Characterization of rHV-GFP *in vitro*. (A) To determine attachment and internalization, PAMs were inoculated with HV or rHV-GFP at an MOI of 1.0 at 4 °C for 1 h. Then the inoculum was removed and cells were washed with medium to remove residual viruses. After 3 h incubation at 37 °C, cellular RNA was isolated and reverse transcribed. Then PCR was performed to identify gene-deleted genomes. (B) rHV-GFP replication was analyzed by detecting the expression of GFP and viral N protein using immunofluorescence assay at 24 h.p.i. (C) The growth curves of parental viruses and the recombinant rHV-GFP were drew by assaying the viral titers of the cell culture supernatants harvested at the indicated time points (12, 24, 36, and 48 h) post-infection by a standard $TCID_{50}$ assay. $^{*}p < 0.05$ between rHV-GFP and the other two viruses, respectively. (D) Representative images of cell death induced by parental viruses and rHV-GFP at 36 h.p.i. PAMs were stained by trypan blue. Magnification, 200×. (E) Cell death rates at 36 h.p.i. were determined by trypan blue exclusion dye staining. $^{***}p < 0.001$, $^{**}p < 0.01$.

To further confirm that viral gene deletion is due to the introduction of an additional TRS6, another viral cDNA clone containing GFP and a copy of TRS2 was constructed (Fig. 3A). RNA recombination was examined by PCR as described above. As shown in Fig. 3B, one band about 3.8 kb was detected in the amplification products from rHV-GFP-TRS2 passage 0 cDNA. When the rescued virus was passaged twice on PAMs, a large band which was about 3.8 kb and a small band which was about 3.1 kb were observed. Only the 3.1 kb band was detected when amplified from passage 5 cDNA. Sequencing analysis of the small band showed that the GFP gene and a copy of TRS2 (779 bp) were deleted and the resulting sequence was exactly the same as that of the wild-type HV. Collectively, these data suggested that RNA recombination was prone to happen after inserting an additional transcriptional unit.

3.3. *rHV-GFP was attenuated both in vitro and in vivo*

As TRS6-insertion resulted in viral structural protein-encoding gene deletion, then we tested its effects on the dynamics of virus replication. Gene-deleted genomes were detected in rHV-GFP infected PAMs in a single replication test (Fig. 4A), indicating that the deletion mutants retained the ability of attachment and internalization. Immunofluorescence assay showed that some GFP negative cells were still viral N protein positive, suggesting that the deletion mutants retained the ability to replicate single cycle and express the remaining viral proteins (Fig. 4B). Then, we examined the kinetics of virus growth in PAMs. As shown in Fig. 4C, the growth curve of rHV was indistinguishable from that of wild-type HV, and virus titers were peaked at 36 h.p.i., whereas TRS6-insertion made rHV-GFP replicated slower than both HV and rHV. rHV-GFP titer at 36 h.p.i. was about six-fold and four-fold lower than that of HV and rHV, respectively, and its titer peak was delayed to 48 h.p.i.. Moreover, trypan blue exclusion dye staining showed that rHV-GFP induced less cell death (Fig. 4D). Cell death rate of PAMs induced by either HV or rHV infection at 36 h.p.i. was about 25%, while the cell death rate induced by rHV-GFP infection was only 8.5% (Fig. 4E).

To further evaluate the pathogenicity of rHV-GFP, pigs were intranasally inoculated with HV, rHV, or rHV-GFP, respectively. Pigs infected with HV or rHV succumbed to the infection within 12 days and showed clinical signs including high fever, coughing, dyspnoea, anorexia, chemosis, shivering, lameness, and skin cyanopathy (Fig. 5A). High rectal temperature (above 40 °C) could be detected as early as 2 days after infection with either HV or rHV in two of the three pigs. The average rectal temperature remained higher than 40.5 °C from day 6 after HV infection and day 4 post rHV infection, respectively (Fig. 5B). In contrast, only one pig infected with rHV-GFP died at 21 d.p.i., while the other three pigs survived (Fig. 5A). However, the cause of death was not clear because it did not show typical syndromes of HP-PRRS. An indirect effect mediated by the high incidence of secondary infections in pigs exposed

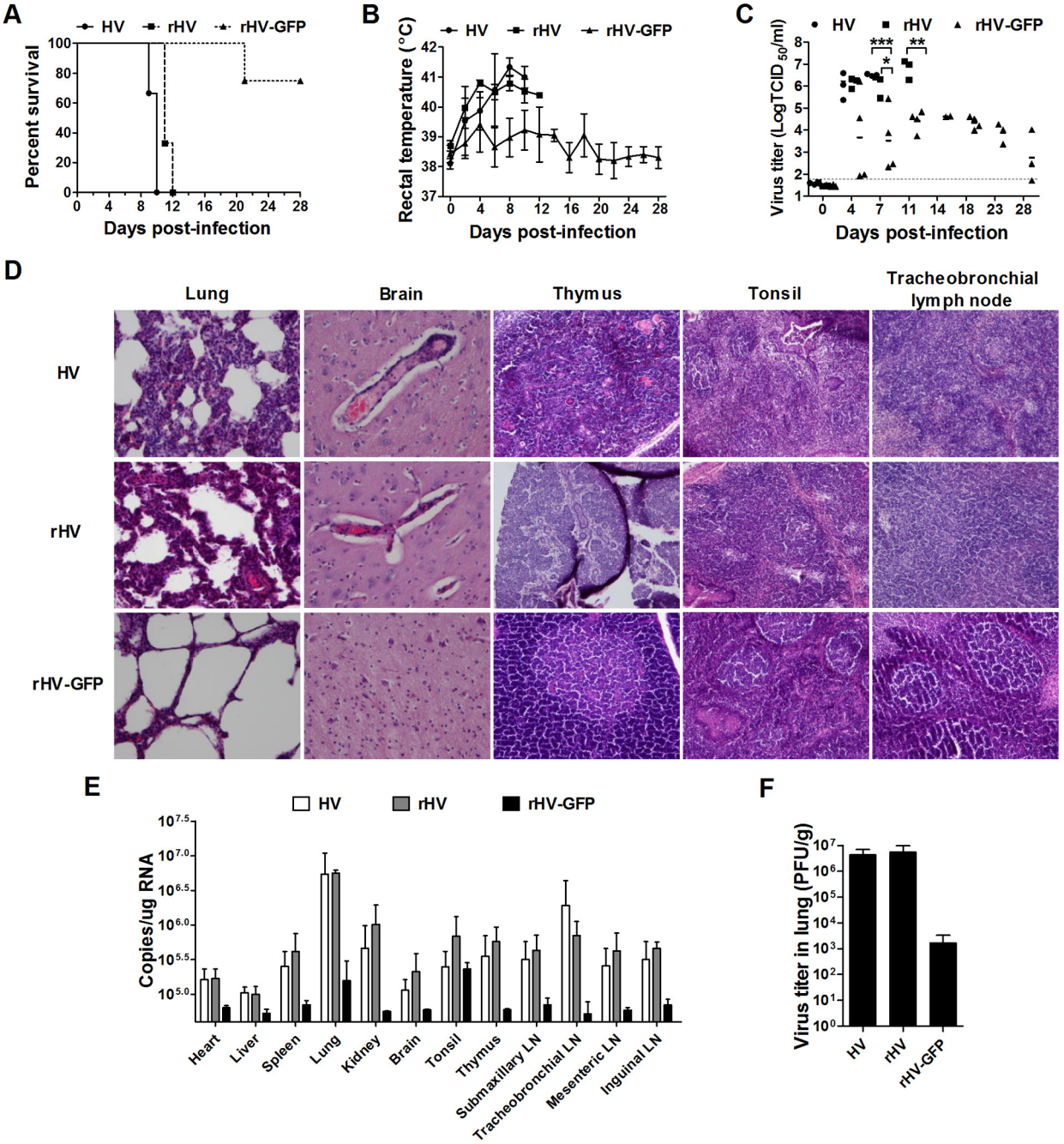

Fig. 5. rHV-GFP is highly attenuated *in vivo*. Pigs were intranasally inoculated with either HV, rHV, or rHV-GFP at 2×10^7 $TCID_{50}$. Survival of pigs (A), rectal temperatures (B), and serum virus titers (C) were monitored. The limit of serum virus titers detection is indicated by dashed line. Tissues collected at autopsy were fixed in 10% neutral-buffered formalin and routinely processed for histological examination, magnification at 200× (D), or snap-frozen in liquid nitrogen and used for virus titers determination (E). LN, lymph node. (F) Viruses isolated from infected lungs were titrated and results were reported in pfu per gram of tissue. $^{***}p < 0.001$, $^{**}p < 0.01$, $^{*}p < 0.05$.

to HP-PRRSV might play a critical role in its death [25]. Two of four pigs infected with rHV-GFP transiently reached 40 °C and 40.2 °C at 4 d.p.i., respectively. The average rectal temperature remained below 40 °C through the experimental period (Fig. 5B).

High levels of viruses were detected at 4 d.p.i. in sera of all HV and rHV infected pigs (range from 2.4×10^5 to 3.8×10^6 $TCID_{50}$/ml, and from 7.8×10^5 to 2.2×10^6 $TCID_{50}$/ml, respectively), whereas virus titers of two rHV-GFP infected pigs were negligible (less than 100 $TCID_{50}$/ml) at 4 d.p.i (Fig. 5C). At 11 d.p.i., serum virus titers of rHV-GFP infected pigs were still 244-fold lower than that of rHV group. At the end of the experiment, virus was eliminated in one of the rHV-GFP infected pigs (Fig. 5C). Severe histopathogenic damages were observed in all HV and rHV infected pigs including severe proliferative interstitial pneumonia in the lung; severe degrees of vasculitis in the brain; blurred white medulla, hyperplastic red medulla in the spleen; collapse of follicles, depletion of germinal centers in the tonsil, and lymph nodes. Both HV and rHV-infected pigs had thymic lesions of cortical involution, causing a poor demarcation between the cortical and medullary zones. No obvious histopathologic damages other than mild interstitial pneumonia were observed in rHV-GFP infected pigs (Fig. 5D). Virus titers in multiple tissues were tested by real-time PCR (Fig. 5E). Results showed that virus titers of rHV-GFP infected pigs remained at significantly lower levels than that of HV and rHV infected pigs

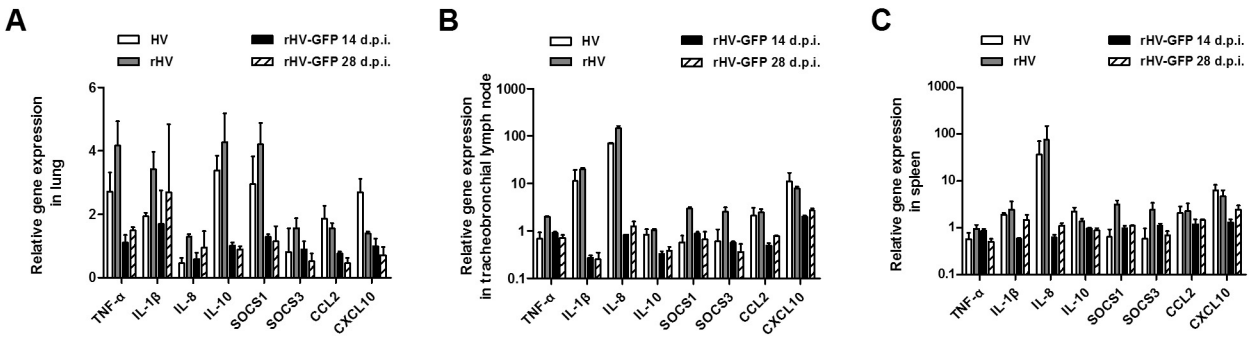

Fig. 6. Effects of attenuation on cytokine and chemokine production. Representative cytokine and chemokine expression in PRRSV infected lungs (A), tracheobronchial lymph nodes (B), and spleens (C) were determined by real-time PCR.

(range from 2-fold to 37-fold), except that tonsil was still a reservoir for rHV-GFP. Notably, virus titers in rHV-GFP infected lungs were about 35-fold lower than that of either HV or rHV infection. Virus isolation was also performed from virus infected lungs, and virus titers of rHV-GFP infected pigs were about 1000-fold lower than that of either HV or rHV infection. Taken together, these data demonstrated that rHV-GFP was remarkably attenuated.

3.4. Effects of attenuation on cytokine and chemokine production

Immunity and immunopathology to viruses are the pros and cons to decide the outcome of the host [26]. In severe acute respiratory syndrome (SARS) patients, cytokines such as IL-1, IL-6, and IL-12, and chemokines such as IL-8, CCL2, and CXCL10 were elevated [27]. The association between the elevated cytokines levels and the severe morbidity and high mortality could also be observed in United States swine experimentally infected by an HP-PRRSV strain [25]. In this study, TNF-α and CCL2 were at least two-fold higher in HV and rHV infected lungs than that in rHV-GFP infected lungs. Anti-inflammatory factor IL-10 and SOCS1 were also higher during HV and rHV infection (Fig. 6A). In lymphoid organs, rHV-GFP infection induced significantly lower levels of IL-1β, IL-8, CCL2, and CXCL10 in tracheobronchial lymph node (range from 3-fold to 176-fold), and more than 33-fold lower of IL-8 in spleen than those in HV-infected pigs (Fig. 6B and C). The decreased cytokine and chemokine expressions during rHV-GFP infection might contribute to the fact that pigs survived with no or only mild pathological lesions.

4. Discussion

In this study, HP-PRRSV strain HV was attenuated due to RNA recombination through introduction of an additional transcription unit. The recombinant rHV-GFP replicated significantly slower than both HV and rHV in PAMs, and the virulence was highly attenuated *in vivo*.

In a previous study in which a similar PRRSV gene expression vector was generated, the authors speculated that potential homologous RNA recombination between the copy of TRS6 and the authentic TRS6 would result in an ORF2-5-deleted virus [10]. In our study, RNA recombinations were identified not only between the additional TRS6 and the authentic TRS6, but also between the inserted foreign gene GFP and ORF4/5. This finding was in accordance with the assumption that RNA recombination might be driven by similar factors and/or signals as discontinuous transcription in nidoviruses [1]. In subgenomic mRNAs synthesis process which resembles similarity-assisted RNA recombination, several noncanonical TRSs have been identified as leader-body junction sites [28,29]. Moreover, insertion of foreign sequence promoted the utilization of TRS-like sequence within the inserted gene and cryptic TRS-like sequences that remained non-functional in native virus [30,31]. In a previous study [32], a replication-competent equine arteritis virus (EAV) expressing GFP via an extra subgenomic mRNA was constructed and leader-to-body junction sites were also found within the GFP gene. Gradual accumulation of viral mutants carrying deletions in the GFP gene was also observed. Further studies need to be done to investigate the influence of other TRS duplication on the frequency of RNA recombination.

The recombinant rHV-GFP replicated significantly slower than both HV and rHV in PAMs. This is in consistent with the previous study [10], in which the authors showed that the replication of P129-GFP was slower than that of wild-type P129 at passages 1–3. However, they showed that the clinical signs of PRRS were comparable in wild-type strain and foreign gene (GFP or capsid protein gene of porcine circovirus type 2) inserted recombinant viruses infected pigs. As wild-type P129 strain only cause mild clinical signs in infected pigs [10,33], we assume that it might be hard to observe the different clinical syndromes between the wild-type P129 and the manipulated strains. Interestingly, in another study attenuated symptoms were also observed when foreign gene IL-1β was expressed from an additional transcriptional product, although the authors initially hypothesized that the recombinant virus might be more virulent than the parental virus because of the continued expression of the proinflammatory cytokine [33].

The deletion mutants of rHV-GFP resemble defective interfering (DI) virus which is defined as a spontaneously generated virus mutant, in which a critical part of the virus genome has been deleted. Naturally occurring DI RNAs have been identified for both arteriviruses and coronaviruses [34,35]. For PRRS virus, the DI-like RNAs are also proposed as “heteroclite RNA” [36–38]. It has been assumed that the DI virus acts as a competitive inhibitor of the complete functional virus (often referred to as the ‘helper’ virus) as DI virus can strongly reduce the yield of helper virus in a mixed infection. In some cases, DI virus has also been observed to attenuate disease in virus-infected animals [39]. In our study, the introduction of an additional TRS6 and foreign gene GFP facilitated the copy-choice template switching and resulted in high-frequency of similarity-assisted RNA recombination. The deletion mutants have retained the essential cis-acting signals for RNA synthesis and viral encapsidation that located in the termini of the genome. When co-infected with wild-type virus with full-length genome, the subsistence of the large number of gene-deleted mutants is largely dependent on complementation of virions with full-length genome, and thus would sequester limiting factor such as viral polymerase components or essential host proteins, and then reduce the viral load of the virulent wild-type virus by interfering the RNA synthesis and virus packaging [38,39]. This might be the possible mechanism accounting for the attenuation of rHV-GFP.

Taken together, our findings demonstrated that additional transcription unit insertion would promote genome instability and

attenuation of HP-PRRSV. However, due to the inherent instability of the recombinant virus population, a full investigation should be performed before this approach can be used in developing expression/vaccine vector.

Conflict of interest

The authors have declared that no competing interests exist.

Acknowledgments

The authors thank Weiquan Liu (China Agricultural University, China) for his helpful suggestions. This work was supported by the National Natural Science Foundation of China (#30770101), and the Faculty Starting Grant and State Key Laboratory of Agrobiotechnology (Grant 2010SKLAB06-1 and 2012SKLAB01-6), China Agricultural University, China.

References

[1] Pasternak AO, Spaan WJ, Snijder EJ. Nidovirus transcription: how to make sense? JGen Virol 2006;87:1403–21.
[2] Fang Y, Snijder EJ. The PRRSV replicase: exploring the multifunctionality of an intriguing set of nonstructural proteins. Virus Res 2010;154:61–76.
[3] Pasternak AO, Gultyaev AP, Spaan WJ, Snijder EJ. Genetic manipulation of arterivirus alternative mRNA leader-body junction sites reveals tight regulation of structural protein expression. J Virol 2000;74:11642–53.
[4] Benfield DA, Nelson E, Collins JE, Harris L, Goyal SM, Robison D, et al. Characterization of swine infertility and respiratory syndrome (SIRS) virus (isolate ATCC VR-2332)s. J Vet Diagn Investig: Off Publ Am Assoc Vet Lab Diagn Inc 1992;4:127–33.
[5] Done SH, Paton DJ. Porcine reproductive and respiratory syndrome: clinical disease, pathology and immunosuppression. Vet Rec 1995;136:32–5.
[6] Li Y, Wang X, Bo K, Tang B, Yang B, Jiang W, et al. Emergence of a highly pathogenic porcine reproductive and respiratory syndrome virus in the Mid-Eastern region of China. Vet J 2007;174:577–84.
[7] Tian K, Yu X, Zhao T, Feng Y, Cao Z, Wang C, et al. Emergence of fatal PRRSV variants: unparalleled outbreaks of atypical PRRS in China and molecular dissection of the unique hallmark. PloS One 2007;2:e526.
[8] Zhou YJ, Hao XF, Tian ZJ, Tong GZ, Yoo D, An TQ, et al. Highly virulent porcine reproductive and respiratory syndrome virus emerged in China. Transbound Emerg Dis 2008;55:152–64.
[9] Snijder EJ, Meulenberg JJ. The molecular biology of arteriviruses. J Gen Virol 1998;79(Pt 5):961–79.
[10] Pei Y, Hodgins DC, Wu J, Welch SK, Calvert JG, Li G, et al. Porcine reproductive and respiratory syndrome virus as a vector: immunogenicity of green fluorescent protein and porcine circovirus type 2 capsid expressed from dedicated subgenomic RNAs. Virology 2009;389:91–9.
[11] Wang C, Huang B, Kong N, Li Q, Ma Y, Li Z, et al. A novel porcine reproductive and respiratory syndrome virus vector system that stably expresses enhanced green fluorescent protein as a separate transcription unit. Vet Res 2013;44:104.
[12] Yoo D, Welch SK, Lee C, Calvert JG. Infectious cDNA clones of porcine reproductive and respiratory syndrome virus and their potential as vaccine vectors. Vet Immunol Immunopathol 2004;102:143–54.
[13] Sang Y, Shi J, Sang W, Rowland RR, Blecha F. Replication-competent recombinant porcine reproductive and respiratory syndrome (PRRS) viruses expressing indicator proteins and antiviral cytokines. Viruses 2012;4:102–16.
[14] Hou J, Wang L, Quan R, Fu Y, Zhang H, Feng WH. Induction of interleukin-10 is dependent on p38 mitogen-activated protein kinase pathway in macrophages infected with porcine reproductive and respiratory syndrome virus. Virol J 2012;9:165.
[15] Hou J, Wang L, He W, Zhang H, Feng WH. Highly pathogenic porcine reproductive and respiratory syndrome virus impairs LPS- and poly(I:C)-stimulated tumor necrosis factor-alpha release by inhibiting ERK signaling pathway. Virus Res 2012;167:106–11.
[16] Lee C, Calvert JG, Welch SK, Yoo D. A DNA-launched reverse genetics system for porcine reproductive and respiratory syndrome virus reveals that homodimerization of the nucleocapsid protein is essential for virus infectivity. Virology 2005;331:47–62.
[17] Wang L, Zhang H, Suo X, Zheng S, Feng WH. Increase of CD163 but not sialoadhesin on cultured peripheral blood monocytes is coordinated with enhanced susceptibility to porcine reproductive and respiratory syndrome virus infection. Vet Immunol Immunopathol 2011;141:209–20.
[18] Zuker M. Mfold web server for nucleic acid folding and hybridization prediction. Nucl Acids Res 2003;31:3406–15.
[19] De Rijk P, Wuyts J, De Wachter R. RnaViz 2: an improved representation of RNA secondary structure. Bioinformatics 2003;19:299–300.
[20] Delrue I, Van Gorp H, Van Doorsselaere J, Delputte PL, Nauwynck HJ. Susceptible cell lines for the production of porcine reproductive and respiratory syndrome virus by stable transfection of sialoadhesin and CD163. BMC Biotechnol 2010;10:48.
[21] Bi Y, Guo XK, Zhao H, Gao L, Wang L, Tang J, et al. Highly pathogenic porcine reproductive and respiratory syndrome virus induces prostaglandin E2 production through cyclooxygenase 1, which is dependent on the ERK1/2-p-C/EBP-beta pathway. J Virol 2014;88:2810–20.
[22] Meulenberg JJ, Bos-de Ruijter JN, van de Graaf R, Wensvoort G, Moormann RJ. Infectious transcripts from cloned genome-length cDNA of porcine reproductive and respiratory syndrome virus. J Virol 1998;72:380–7.
[23] Baird HA, Galetto R, Gao Y, Simon-Loriere E, Abreha M, Archer J, et al. Sequence determinants of breakpoint location during HIV-1 intersubtype recombination. Nucl Acids Res 2006;34:5203–16.
[24] Simon-Loriere E, Holmes EC. Why do RNA viruses recombine? Nat Rev Microbiol 2011;9:617–26.
[25] Guo B, Lager KM, Henningson JN, Miller LC, Schlink SN, Kappes MA, et al. Experimental infection of United States swine with a Chinese highly pathogenic strain of porcine reproductive and respiratory syndrome virus. Virology 2013;435:372–84.
[26] Rouse BT, Sehrawat S. Immunity and immunopathology to viruses: what decides the outcome? Nat Rev Immunol 2010;10:514–26.
[27] Perlman S, Netland J. Coronaviruses post-SARS: update on replication and pathogenesis. Nat Rev Microbiol 2009;7:439–50.
[28] Meng XJ, Paul PS, Morozov I, Halbur PG. A nested set of six or seven subgenomic mRNAs is formed in cells infected with different isolates of porcine reproductive and respiratory syndrome virus. J Gen Virol 1996;77(Pt 6):1265–70.
[29] Hussain S, Pan J, Chen Y, Yang Y, Xu J, Peng Y, et al. Identification of novel subgenomic RNAs and noncanonical transcription initiation signals of severe acute respiratory syndrome coronavirus. J Virol 2005;79:5288–95.
[30] Zheng H, Sun Z, Zhu XQ, Long J, Lu J, Lv J, et al. Recombinant PRRSV expressing porcine circovirus sequence reveals novel aspect of transcriptional control of porcine arterivirus. Virus Res 2010;148:8–16.
[31] Sola I, Alonso S, Zuniga S, Balasch M, Plana-Duran J, Enjuanes L. Engineering the transmissible gastroenteritis virus genome as an expression vector inducing lactogenic immunity. J Virol 2003;77:4357–69.
[32] de Vries AA, Glaser AL, Raamsman MJ, Rottier PJ. Recombinant equine arteritis virus as an expression vector. Virology 2001;284:259–76.
[33] Lawson SR, Li Y, Patton JB, Langenhorst RJ, Sun Z, Jiang Z, et al. Interleukin-1β expression by a recombinant porcine reproductive and respiratory syndrome virus. Virus Res 2012;163:461–8.
[34] Molenkamp R, Rozier BC, Greve S, Spaan WJ, Snijder EJ. Isolation and characterization of an arterivirus defective interfering RNA genome. J Virol 2000;74:3156–65.
[35] Makino S, Taguchi F, Fujiwara K. Defective interfering particles of mouse hepatitis virus. Virology 1984;133:9–17.
[36] Yuan S, Murtaugh MP, Schumann FA, Mickelson D, Faaberg KS. Characterization of heteroclite subgenomic RNAs associated with PRRSV infection. Virus Res 2004;105:75–87.
[37] Yuan S, Murtaugh MP, Faaberg KS. Heteroclite subgenomic RNAs are produced in porcine reproductive and respiratory syndrome virus infection. Virology 2000;275:158–69.
[38] Xiao CT, Liu ZH, Yu XL, Ge M, Li RC, Xiao BR, et al. Identification of new defective interfering RNA species associated with porcine reproductive and respiratory syndrome virus infection. Virus Res 2011;158:33–6.
[39] Marriott AC, Dimmock NJ. Defective interfering viruses and their potential as antiviral agents. Rev Med Virol 2010;20:51–62.